

# Analysis of Aperture Evolution in a Rock Joint Using a Complex Network Approach<sup>1</sup>

Hamed .O.Ghaffari & Mostafa.Sharifzadeh

*Department of Mining & Metallurgical Engineering, Amirkabir University of Technology, Tehran, Iran*

**Abstract:** In this study, we develop a complex network approach on a rough fracture, where evolution of elementary aperture during translational shear is characterized. In this manner, based on the Euclidean measure, we make evolutionary networks in two directions (in parallel and perpendicular to the shear direction) and on the measured apertures' profiles. Evaluation of the emerged networks shows the connectivity degree (distribution) of networks, after a transition step; fall in to the stable states which are coincided with the Gaussian distribution. Based on this event, we present a model in which evolving (decaying) of networks are accomplished using a preferential detachment (based on certain probability) of edges. Also, evolving of cluster coefficients and number of edges displays similar patterns as well as are appeared in shear stress and dilation changes, respectively.

**Keywords:** *Complex Network, Aperture Evolution, Rock Joint*

## 1. Introduction

Understanding of rock joint behaviors, either in single or swarm form, under the several natural or artificial forces has allocated numerous researches during the evolution of rock mechanics field. Scientists have shed light on the several approaches to capture interacted rock joint(s) manners as well as analytical solutions to hybrid numerical methods and the methods based upon indirect investigations such as fractal , statistical or natural based computing methods [1]-[3]. Rock joint performance as a result of collective behavior of the constructed elements (say fraction/pixel in each surface), interacting with each other, determines nonlinear picture of a changeable system. Obviously, one cannot predict the rich behavior of the whole by merely extrapolating from the treatment of its units [23].

---

**1 .The paper has been submitted to International Journal of Rock Mechanics & Mining Sciences**

1 This is a prevalent gesture of complex systems. The success in describing of interwoven  
2 systems using physical tools as a major reductionism is associated with the simplifications of  
3 the interactions between the elements so that complexity reduction is a rescue pathway to  
4 regulation of approximated analyses of collective particles having swing states, complicated  
5 structures, and diversity of relations among elements. Dissection of phenomena under  
6 investigation into a list of interacting unites- which are building blocks (granules) of system-  
7 connected by pair-wise connections, can be revealed in complex networks, which provide a  
8 mathematical framework to analysis of wide range of complex systems. Picturing, modeling  
9 and evaluation in a simple and intuitive way are some of the discriminated features of  
10 complex networks [4],[5].Complex networks have been developed in the several fields of  
11 science and engineering for example social, information, technological, biological and  
12 earthquake networks are the main distinguished networks [6]-[9].

13 On the other hand, to catch on Hydro-mechanical and mechanical behavior of a rock  
14 joint, domination on to the surface morphology evolution as well as aperture is irrefutable. In  
15 this way, characterization of aperture of a rock fracture has been realized by using several  
16 techniques such assigning of probability distributions (random field theory) [1], [2] and –  
17 [11], [12] correlation length [14], fractals [13] and spatial correlation (semi-variograms) [3]. In  
18 this study, we provide a complex network approach on the aperture evolution during  
19 transitional shear accounting in two separated directions of shear while the disclosed  
20 networks involve the inherent difficulties such dynamical concepts of components, changing  
21 the wiring diagrams and meta- complications. Also, upon the consequences we present an  
22 algorithm, offering a general view of transitions of an elementary aperture distribution, which  
23 its main core is associated by preferential detaching of similar granules. In addition to these  
24 procedures, the mechanical properties and hydraulic conductivity of the being joint are  
25 compared with the networks properties.

26 The first part of this article covers the employed method, some preliminary aspects of  
27 networks measurements, and the proposed algorithm on the real results accompanying an  
28 analytical solution for the algorithm. The next section includes the results obtained from the  
29 experimental tests on a rock joint and the arranged complex networks. In discussion part, we  
30 investigate other types of similarity measures -to construction of networks edges-which

1 exhibit other sides of a rock joint evolution, the affections of contacts zones and their  
 2 variations at the successive displacements.

### 3 **2. Method**

4 A network (graph) consists of nodes and edges connecting them [20]. In this study our  
 5 aim is to setting up of a network approach on the measured apertures' profiles so that  
 6 characterization of the appropriate aperture behavior under the successive shear  
 7 displacements is accomplished. To set up a network on the aperture patterns, we consider  
 8 each aperture profile<sup>2</sup> as a node, so named profile-profile network (Fig.1). To make edge  
 9 between two nodes, a relation should be defined. In this study we focus on the similarity  
 10 measure between nodes while two mathematical measures are employed: Euclidean  
 11 distance as a core of our networks and Chebyshev (the  $L_\infty$  metric) as a complementary  
 12 metric, which are given as below, respectively [24]:

$$13 \quad d_{Eucl.} = \sqrt{\sum_{p,q=1:n_p} (p(x_1, x_2, \dots, x_n) - q(x_1, x_2, \dots, x_n))^2} \quad , \quad (1)$$

$$14 \quad d_{Che.} = \max_i (|x_i^p - x_i^q|) = \lim_{k \rightarrow \infty} \left( \sum_{i=1}^n |x_i^p - x_i^q|^k \right)^{\frac{1}{k}} \quad , \quad (2)$$

15 where  $p$  and  $q$  are the  $i^{th}$  profiles and  $x_k^i (i \in \{p \vee q\})$  shows  $k^{th}$  element from the  
 16  $i^{th}$  profile. It must be noticed the Chebyshev distance returns the maximum distance  
 17 between elements in the assumed profiles. When  $d \leq \xi$  an edge among two nodes is  
 18 created. As it can be seen the emerged networks upon the mentioned way are undirected

---

2-X-profiles: apertures' profiles parallel with the Y-axis (perpendicular to the shear direct) and Y-profiles are parallel with the shear direct.

1 networks. The threshold  $\xi$  depicts error level, usually can be assumed as 5-20 percent of  
 2 maximum  $d$  (Here we put  $\approx 5$  for Euclidean distance). In the other view and based on  
 3 granularity [17], [18] of the collected information, choosing of such constant value may be  
 4 associated with the current accuracy at data accumulation where after a maximum  
 5 threshold the system (here apertures evolution) lose its dominant order. In the parallel with  
 6 this discussion, scaling or categorization of the appeared apertures (points) shows a similar  
 7 procedure so that distribution transition from a binomial state (when we don't consider  
 8 variation of apertures values) to other multi-bins cases (which are similar to the feature)  
 9 can be observed. This proves how discretization of an event displays different and  
 10 sometimes contradictive faces of dynamical systems.

11 Let us introduce some properties of the undirected networks: clustering coefficient  
 12 ( $C$ ) and the degree distribution ( $P(k)$ ). The clustering coefficient describes the degree to  
 13 which  $k$  neighbors of a particular node are connected to each other. Our mean about  
 14 neighbors is the connected nodes to the particular node. To better understanding of this  
 15 concept the question "are my friends also friends of each other?" can be used. In fact  
 16 clustering coefficient shows the collaboration (or synchronization and tendency) between  
 17 the connected nodes to one. Assume the  $i^{th}$  node to have  $k_i$  neighboring nodes. There can  
 18 exist at most  $k_i(k_i - 1)/2$  edges between the neighbors (local complete graph). Define  $c_i$   
 19 as the ratio

$$20 \quad c_i = \frac{\text{actual number of edges between the neighbors of the } i^{th} \text{ node}}{k_i(k_i - 1)/2} \quad (3)$$

21 Then, the clustering coefficient is given by the average of  $c_i$  over all the nodes in the  
 22 network:

$$C = \frac{1}{N} \sum_{i=1}^N c_i. \quad (4)$$

For  $k_i \leq 1$  we define  $C \equiv 0$ . The closer  $C$  is to one the larger is the interconnectedness of the network. The connectivity distribution (or degree distribution),  $P(k)$  is the probability of finding nodes with  $k$  edges in a network. In large networks, there will always be some fluctuations in the degree distribution. The large fluctuations from the average value ( $\langle k \rangle$ ) refers to the highly heterogeneous networks while homogeneous networks display low fluctuations. The mentioned properties of large networks (and so other measures [4], [5] and [7]) make the relatively analysis of the possible statistical properties of such networks. By using these attributes, we can manifest the underlying laws that govern the evolution of the complex networked systems.

There are different types of the networks models which have been developed based on specific events in the real world, for instance the Erdos-Renyi (random)[20], the small-world ( Watts-Strogatz model[8],[10] ), and the scale-free (Albert-Barabasi model) models [5],[6]. In this part of this study and upon the observed emerged behavior of the covered networks on the apertures' profiles (section results), we present a simple model which considers the edges detachments (decaying of initial similarity patterns) of the networks. So, using a continuous analysis the behavior of the proposed algorithm is proved. For simplicity, our model doesn't take in to account the nodes decaying (as it comes out in the X-profiles evolving) and attempt to capture the nearly possible mechanism(s) that govern the evolution of network topology, guided by the real information involved in the degree distribution. Our algorithm is another changed version of the limiting case of the scale-free model [5], [6] where the decaying of network is ignored. The steps of the algorithm are as follows:

- 1) Starting with  $N$  nodes (number of profiles) and like real initial state of a joints 'profiles, construct a fully connected graph (lattice network) where all of nodes are connected except a few of them.
- 2) At each time step, select a node uniformly and detach the edge which its end point (node  $i$  with the degree  $k_i$ ) is selected with a preferential probability ,is given as:

$$\Pi(k_i) = \frac{k_i}{\sum k_j},$$

where the sum in the denominator goes over all nodes in the system except the source node. The change rate of node connectivity has two components: the first describes the probability that node  $i$  is chosen randomly as:  $\Pi_{random}(k_i) = 1/N$  and the second is related with  $\Pi(k_i) = \frac{k_i}{\sum k_j}$ , regulating the probability that an edge beginning from a randomly selected node is detached from node  $i$  :

$$\frac{\partial k_i}{\partial t} = -\left(A \frac{k_i}{\sum_{j=1}^N k_j} + \frac{1}{N}\right) \quad (5)$$

which gives the time dependence of the degree  $k_i$  of an assumed node  $i$  while under this assumption that  $k_i$  is a continuous real variable . Considering  $\sum k_j = N^2 - N - 2t$  and the variation of connectivity during time step is  $\Delta(k) = -2$ , we obtain  $A \approx (2N - 1)$ , so since  $N \gg 1$  then  $A \approx 2N$  .Replacing them at Eq.(5) and solving of this equation is led to the approximated form :

$$k_i(t) \approx \left(N - \frac{2t}{N}\right) \left(1 - \frac{2t}{N^2}\right)^N \quad (6)$$

As one can see the emerged equation shows the similar behavior as it is appeared in real evolution of X or Y apertures' profiles. The main difference with the real observations (results section) is in the very soft transition while occurs at the delayed time. To capture this state, we can change the number of random selection of nodes to the  $m$  times at each step. Fig.2a and b show the evolution of edges frequency obtained from the mentioned algorithm ( $N=90$ ) over the different time step. Fig.2c and d illustrate the variations of the edges ( $\sum k_i$ ) and  $k_i(t)$ -using Eq. (6)-during 2500 and 8000 time steps, respectively. In the other process, by several values of N, Eq. (6) has been portrayed (Fig.3). As it can be seen after

1  $t \approx N^2$  time steps the system reaches a state which all nodes are isolated. It should be noticed  
2 that Eq. (6) is valid only for  $t > t_{\text{int.}}$  where  $t_{\text{int.}}$  is the time when node  $i$  was selected for the  
3 first time as the origin of an edge. So, all nodes follow the aforesaid dynamics after  $t \geq N$  .

4 Also, as if our system cannot capture all of the appeared states of the real complex  
5 networks, but may give an overall view on the designated networks on the apertures  
6 alterations: “*destroying of the high similar profiles (at least in initial steps) associated with a*  
7 *preferential probability*”. It can be proved that removing of the most highly connected nodes  
8 at each step bears the most damaging to the integrity of the system but in this case the system  
9 doesn’t show like behavior in the edges distribution and linear rate of nodes removal [5].  
10 Considering this point that in Y-profiles against X-profiles the number of active (non-  
11 isolated) nodes shows a constant state, the dominant mechanism can be conjectured as a  
12 combining of two processes on the overall profiles (real joint) . One may change the  
13 constructive parts of Eq. (5) to reach more exact results; for instance, considering non-linear  
14 core in the preferential probability or selection/detachment depends on time passing.

### 15 **3. Results**

16 In this part, we focus on the experimental results and mapping them in to the complex  
17 networks. Regard this point that the network anatomy is so important to characterization  
18 (because structure always affects function) our aim is underlined to find out the possible  
19 relations between the constructed networks properties and the current mechanical / hydro-  
20 mechanical properties of a rock joint which is under a constant normal stress and the  
21 successive shear displacements.

22 The rock material was granite with the weight of 25.9 and uniaxial compressive  
23 strength of 172 Mpa. An artificial rock joint was made at mid height of the specimen by  
24 splitting using special joint creating apparatus, which has two horizontal jacks and a  
25 vertical jack [1],[15]. The sides of the joint are cut down after creating joint and its final  
26 size is 180 mm in length, 100 mm in width and 80 mm in height. Using special mechanical

1 units the different mechanical parameters of this sample were measured. A virtual mesh  
 2 having a square element size of 0.2 mm spread on each surface and each position height  
 3 was measured by the laser scanner. Also using a special hydraulic testing unit is employed  
 4 to allow linear flow experiments (parallel with shear direction) to be governed while the  
 5 rock joint is undergoing normal or shear loading. The details of the procedure can be  
 6 followed in [15], [16]. The hydraulic conductivity and hydraulic aperture are given by  
 7 Darcy's law:

$$8 \quad Q = K_h A i, \quad (7)$$

9 and assuming the joint surfaces are as two smooth parallel plates ,the flow rate and hydraulic  
 10 conductivity can be written as below:

$$11 \quad Q = \frac{g e_h^2}{12\nu} (w e_h) i, \quad (8)$$

$$12 \quad K_h = \frac{g e_h^2}{12\nu}, \quad (9)$$

13 where  $Q, A, i, K_h, g, e_h, \nu$  and  $w$  are the volumetric flow, area, hydraulic gradient,  
 14 hydraulic conductivity, the gravity acceleration( $\frac{m}{s^2}$ ),hydraulic aperture, kinematic  
 15 viscosity of fluid and the width of the specimen ,respectively.

16 In this study, we consider only the evolving of apertures under constant normal stress and  
 17 regular translational shear in which the lower surface has fixed position and upper one is  
 18 displaced (Fig.4). By employing a threshold value- $d \leq 5$ - in Euclidian distance (Eq. (1)) and  
 19 setting up a pre-designated complex network (Fig.1a) on the X-profiles, gradual changes of  
 20 the adjutant matrix form of the appeared networks can be inferred (Fig.5). Fig.5 demonstrates  
 21 after a phase transition step the similarities' patterns are constrained to the adjacency of each  
 22 profile. The neighborhood radius –in the final stages of disruption- changes from 2 to 20



1 pixels (0.4-4 mm), except for boundary profiles. The concentration of similarities takes place  
2 around 5-10 pixels where lower and higher values sort in a symmetric shape which disclose a  
3 Gaussian distribution.

4 Portraying total number of edges, number of active nodes (non-isolated sites) and  
5 clustering coefficient, during transitional shear stress, reveals others properties of the  
6 assigned networks. At X-profiles, decreasing of the edges after SD=1 (Fig.6 a) is coincided  
7 with a transition point (interval) which shows the system after an abruptly falling, goes  
8 towards a stable state. This behavior, called phase transition, is a usual and current behavior  
9 in several natural systems such as physical, social and economical systems [18], [21] and  
10 [22].

11 In fact, elicitation , prediction and finding out of effective parameters of phase transition  
12 step(s) are one of the main stages in this track where system goes from a stable (or unstable)  
13 to another stable (or unstable such as social revolutions) and order (disorder) parameter(s)  
14 characterizes these transformation occasions. If we transform  $K$  to the reverse case and re-  
15 plot the overall changes in a log-log coordinates, the general form of a continuous phase  
16 transition is appeared. It must be noticed that the phase alteration in this case is not an order  
17 to disorder (or reverses case) but is a soft transition from an order to the semi-order case where  
18 after 4 mm the system reaches a semi-stable state. We can designate a sigmoid function [22]  
19 and with some mathematical manipulation, is followed as below:

$$20 \quad k = 2 \times 10^5 \times \left( 1 + e^{-\beta \left( 1 + \frac{LnSD}{1 + \delta LnSD} \right)} \right) \quad (10)$$

21 where  $\beta$  and  $\delta$  are the regulator parameters which determine the declining rate (Fig.7). It  
22 should be reminded the proposed algorithm (section 2) represents a similar graph for edges  
23 descending.

24 A similar behavior can be followed in the appropriate Y-profiles where the number of  
25 active nodes has a constant value and doesn't show an intermediate step in declining  
26 procedure (discontinuous transition). Here, the order parameter is selected as the number of  
27 edges which in general form is concurred with the contact percent or normal displacement

1 versus shear displacements (Fig.6.d). This implies that the decreasing of contact zones  
2 induces lower similarities between profiles (unmated) either in X or Y directions. However,  
3 by indenting of contact zones and diminishing of percolation clusters, the proper networks  
4 with the stair-profiles expose interesting property where in first look have a contradictory  
5 manner: emerging of growing networks (refer to the discussion section).

6 Gradual changes of connectivity distributions, either in X or Y profiles, reveals a  
7 similar transitional behavior: transformation from a nearly single value function to a semi-  
8 stable Gaussian distribution (Fig.8). In parallel profiles of networks with shear direction the  
9 neighborhood radius shows a lower interval rather than X-profiles, so-in agree with  
10 connectivity numbers changes- transition to a semi-stable stage is occurred with more  
11 convergence rate. In other word, similarities of Y-profiles occur in higher constraints and  
12 readily (faster than opposite option). The possible reason can be inferred from the lower  
13 resistance against transitional shear (and also easy leading of fluid flow), results more loosing  
14 of possible contacts –increasing percolation clusters-and abrasion of asperities in the Y-  
15 profiles.

16 The complementary results using calculation of clustering coefficients emphasis that  
17 the inverse values of  $C$  during process ,in X-profiles, hand out like pattern as ones came out  
18 in the variations of shear stresses (Fig.9 a and c) while in the same manner and on Y-profiles  
19 resembles with the increment of hydraulic conductivity values (Fig.9 b and d). The  
20 coinciding of  $1/C_Y$  with the changes of the hydraulic conductivity rather than the dilation  
21 behavior proves that the joint un-matching (or increment of mean aperture) is not only  
22 singular parameter in the fluid flow, as if reduction of joint roughness and the entire  
23 ensembles of the similarity behaviors of asperities are other possible agents.

24 Also, these results indicate that lower synchronization in X-profiles causes great  
25 resistance against shear stress and higher orchestration at Y-profiles bears minimum  
26 hydraulic conductivity, particularly at a step that interlocking of (SD=1) asperities and  
27 simultaneously decreasing of flow pathways take place. It should be noticed that the  
28 sensitivity of the clustering coefficients to the scaling is very high ,for instance with 5 and 10  
29 times of virtual meshes (1-2 mm), the details of the  $C$  fluctuations are omitted ,however, the

1 general form of variations is preserved as it is resulted at real experimental outputs [19].

2 The aforesaid discussion can be perused with more details within the inter-structure of  
3 the networks. In first case, consider number of active nodes is constant i.e.

4  $\frac{\partial N}{\partial t} = 0$  (assuming shear distance has a direct relate with time) with the constraints

5  $\frac{\partial K}{\partial t} > 0$  and  $\frac{\partial C}{\partial t} > 0$  that indicates new edges are added to the system in the manner that the

6 attached edges increase the collaboration of nodes, especially when  $\frac{\partial C}{\partial t} > \frac{\partial K}{\partial t}$  the

7 connections are concentrated in to the “friends” nodes (rewiring within collaborated clusters).

8 In other word, the synchronization between the neighborhoods nodes is promoted. In another

9 aspect, when we have  $\frac{\partial C}{\partial t} \approx \frac{\partial K}{\partial t}$ , implies on the uniform edges growing between vertices.

10 For a reverse position ( $\frac{\partial C}{\partial t} < \frac{\partial K}{\partial t}$ ), the most added edges extends in out of friends nodes

11 ranges, i.e. the nodes are linked to new other sites. A similar argument can be followed on the  
12 other cases [19].

#### 13 **4. Discussion**

14 In this section, we investigate the sensitivity of the profiles distance to the predefined error  
15 level, the results based on Chebyshev distance and exploring of networks due to the contact  
16 profiles. Selection of error level as a critical factor in elicitation of networks plays a  
17 prominent role. For instance the variation of edges frequency at SD=20 mm depends on  
18 threshold levels ( $(0.5 \leq \xi \leq 8)$ ) pursues an initial exponential, at elementary values, to a  
19 Gaussian at middle values and with increasing of error level looses the latter distribution  
20 (Fig.10). Nevertheless, we can follow like procedure on the connectivity distribution-time  
21 which changes from a single-scale distribution (closer to single value function) to a semi-  
22 stable Gaussian. In fact, the shape of these distributions might result from the presence of  
23 constraints limiting the number of links when connections are costly. In this sense, the  
24 exponential decays (rising) or sharp cutoffs would be a result of highly wiring [7].

1 As before mentioned each vertex or a cluster of nodes in a network presents one or set of  
 2 properties which are connected to each other based on their similarity, functional, spatial or  
 3 temporal proximity properties. These relations are the main foundation of the information  
 4 packaging or elicitation of best briefed “granules” where such information granules uncover  
 5 and constitute the overall and collective behavior of a complex system. Elicitation of such  
 6 packages can be carried out using different, say, similarity measures which will be depends  
 7 upon the problem space. In any information system several parameters can be recognized,  
 8 either in statistical or dynamical systems. These attributes if have same types form a  
 9 homogenous space else a heterogeneous field is produced. In our problem, the nature of  
 10 attributes is apertures which create a multi-dimensional Euclidean space. The Euclidean  
 11 metric can give very different results when the scale of a variable is changed .This problem  
 12 may be elevated by the normalization of all attributes (a weighted Euclidean norm) .Although  
 13 the Euclidean distance is the most common and popular metric in formation of granules but  
 14 other similarity measures exist.

15 The employing of these relations is tied with the problem being solved. Here, we  
 16 investigate two measurements. In first case, the Chebyshev distance (Eq. 2) which is a metric  
 17 related to Euclidean and Manhantan distances is used. In Manhantan distance, the distance is  
 18 computed by summing the absolute value of the difference of individual terms

19  $(d(p,q) = \sum_{i=1}^n |x_i^p - x_i^q|)$  which express the minimum similarity is not always in agreement

20 with Euclidean, especially when there are some restrictions on freely movements in the given  
 21 space. The results shows similar results as one can see in the usage of Euclidean distance  
 22 with some softer behavior in the initially distributions and transition interval (Fig.11) which  
 23 changes from a nearly power-law ( $N(k) \propto k^{-\gamma}$ ) to a single-scale distribution (Gaussian).  
 24 The significant reason can be originated from the Chebyshev definition which the distance  
 25 fall in to the maximum apertures differences, therefore, can’t involve the details of the  
 26 apertures details.

27 In other process and based upon a modified version of binary distance measure, the role  
 28 of contacts zones is distinguished. Instead of pairwise comparison of elements, the Euclidean  
 29 distance is utilized while percolating clusters and contact pixels are transformed in to the 0

1 and 1, respectively (Fig.12). Accomplishing of the profiles networks exhibits the new type of  
2 contacts profiles evolutions: Growing networks either in X or Y profiles (Fig.13).At initial  
3 steps of the evolving, neither active nodes nor edges are appeared. This is due to the high  
4 fluctuations of contact profiles which are in the stair like shapes. The variation of  
5 connectivity distribution shows a transition from an exponential to another type of one.  
6 Particularly, for X-profiles, the emanation of three distinguished zones is clear (Fig.13 a-  
7 inent). Increscent of displacement induces a lower instability of contacts profiles which  
8 impel more similarity (Fig.13 c and d). However, for instance in X-profiles, after a step  
9 (SD=6) developing of new sites are stopped while the growing of edges is continuing. In  
10 addition to this event at  $\frac{\partial N}{\partial t} = 0$  (after SD=5 –compare with Fig.9a and c), we have  
11  $\frac{\partial C}{\partial t} < \frac{\partial K}{\partial t}$  proves the promoting of connectivity with other nodes (are not parts of  
12 collaborative nodes). This interval is coordinated with the reduction of roughness represents  
13 even though the percentage of contacts gets in to a nearly constant value but the similarity of  
14 contact profiles are continuously added (the coherent variation of contacts patterns). It should  
15 be ignoring of contacts is equivalent with distinguishing of percolating areas which in profile  
16 form and based on the mentioned measurement display like behavior of networks related to  
17 the contacts profiles.

## 18 5. Conclusions

19 The success in describing of interwoven systems using physical tools as a major  
20 reductionism is associated with the simplifications of the interactions between the elements  
21 where there is no possible vagueness. Employing of statistical mechanics tools gives a good  
22 framework for analysis of these systems. Also, possible relations between the building blocks  
23 of complex systems can be revealed in complex networks, which describe a wide range of  
24 systems from social systems to grid power systems, earthquake networks to other physical  
25 systems, World Wide Web to citation of papers.

26 From this perspective and by considering of the complicated behavior of a rough fracture  
27 which was under the shear stress, a network associated with a popular similarity measure was

1 designated at two separated directions of the shearing. The networks properties shed light a  
2 suitable coordination with the empirically obtained mechanical and hydro- mechanical  
3 characters of the being joint. Recognition of phase transition step, reforming of inter-  
4 structures evolutions, the weight of perpendicular profiles against resistance and procuring of  
5 great order in parallel profiles are some of the benefits of the captured networks. Also, to  
6 highlight and indent the contacts functionality another bi-partite schema of profiles as  
7 dynamical nodes were taken in to account. The results emphasized on the formation of  
8 contacts clusters (in pick point at shear stress-shear displacement plot) which their similarities  
9 were increased with more ate in X-profiles than the opposite direction, representing growing  
10 networks just unlike the former case.

11 Based on the observations of the decaying apertures' profiles networks, we proposed an  
12 algorithm, regard to the overall performance of the real networks and transformation of  
13 connectivity distribution, which the edges break out were accomplished by preferential  
14 detachments. This may stresses on this point that ,without considering of nodes demolishing,  
15 the starting point of links cutting are more closer to the high dense nodes rather than to  
16 others. Definitely, the represented indirect modeling of the evolving networks is only a start  
17 point which can be extended with high preciseness and regarding more details.

## 18 **References**

- 19 1. Sharifzadeh M. Experimental and theoretical research on hydro-mechanical coupling properties of rock joint. Ph.D.  
20 thesis, Kyushu University, Japan; 2005.
- 21 2. Adler MP and Thovert JF. Fractures and fracture networks. Kluwer Academic; 1999.
- 22 3. Koyama T. Numerical modeling of fluid flow and particle transport in rock fractures during shear, PhD thesis ,Royal  
23 Institute of Technology (KTH),Stockholm, Sweden;2005.
- 24 4. Newman M. E. J. The structure and function of complex networks, SIAM Review 2003; 45(2): 167- 256.
- 25 5. Albert R., Barabasi A.-L. Statistical mechanics of complex networks. Review of Modern Physics 2002; 74, 47–97.
- 26 6. Barabasi A.L, Albert R, Jeong H. Mean–field theory for scale-free random networks,  
27 1999.<http://www.arxiv.org/condmat/9907068v1>
- 28 7. Bomer K, Sanyal S, Vespiganani A. Network's science .In: Annual review of information science & technology 2007;  
29 41(12):537-607.
- 30 8. Watts DJ, Strogatz SH. Collective dynamics of small-world networks. Nature 1998; 393:440-442
- 31 9. Abe S, Suzuki N. Complex network description of seismicity . Nonlin process Geophys 2006;13:145-150
- 32
- 33
- 34
- 35
- 36
- 37
- 38
- 39
- 40

- 1 10. Strogatz,S.H. Exploring complex networks, Nature. 2001; Vol .410:268-276.
- 2
- 3 11. Hakami E, Einstein H H,Genitier S , Iwano M. Characterization of fracture apertures-methods and parameters. In: Proc
- 4 of the 8<sup>th</sup> Int Congr on Rock Mech, Tokyo, 1995: 751-754.
- 5
- 6 12. Lanaro F, Stephansson O.A. Unified model for characterization and mechanical behavior of rock fractures. Pure Appl
- 7 Geophys,2003;160:989-998
- 8
- 9 13. Lanaro F.A. Random field model for surface roughness and aperture of rock fractures. Int J Rock Mech Min Sci, 2000,
- 10 37:1195-1210.
- 11
- 12 14. Brown SR, Kranz RL , Bonner BP. Correlation between the surfaces of natural rock joints, Geophys Res Lett, 1986;
- 13 13(13):1430-1433.
- 14
- 15 15. Sharifzadeh M, Mitani Y, Esaki T, Urakawa F. An investigation of joint aperture distribution using surface asperities
- 16 measurement and GIS data processing. Asian Rock Mechanics Symposium (ARMS3), Mill Press, Kyoto, 2004:165–
- 17 171.
- 18
- 19 16. Sharifzadeh M, Mitani Y, Esaki T. Rock joint surfaces measurement and analysis of aperture distribution under
- 20 different normal and shear loading using GIS , Rock Mech. Rock Engng. 2006; DOI 10.1007/s00603-006-0115-6.
- 21
- 22 17. Ghaffari O.H, Sharifzadeh M, Shahrair K. and PedryczW. Application of soft granulation theory to permeability
- 23 analysis, Int J Rock Mech Mining Sci, 2008;doi:10.1016/j.ijrmms.2008.09.001.
- 24
- 25 18. Ghaffari O.H, Sharifzadeh M, Pedrycz W. Phase transition in SONFIS and SORST, In RSCTC 2008, LNAI 5306, eds.
- 26 C.-C. Chan et al. 2008:339 – 348.Springer-Verlag: Berlin Heidelberg.
- 27
- 28 19. Ghaffari O.H. Applications of intelligent systems and complex networks in analysis of hydro- mechanical coupling
- 29 behavior of a single rock joint under normal and shear Load. M.Sc Thesis, Amirkabir University of Technology,
- 30 Tehran, Iran; 2008.
- 31
- 32 20. Wilson RJ. Introduction to graph theory. Fourth Edition: Prentice Hall, Harlow; 1996.
- 33
- 34 21. Millonas M.M. Swarms, phase transitions, and collective intelligence, 1993: <http://arxiv.org/abs/adap->
- 35 [org/9306002](http://arxiv.org/abs/adap-org/9306002).
- 36
- 37 22. Levy M. Social phase transitions. Journal of Economic Behavior& Organization 2005; 57:71–87.
- 38
- 39 23. Hakan H. Synergetics: An Introduction. Springer, New York; 1983.
- 40
- 41 24. Bezdek JC, Keller J,Krisnapuram R , Nikhil RP. Fuzzy models and algorithms for pattern recognition and image
- 42 processing. Springer;2005.
- 43
- 44
- 45

## Analysis of Aperture Evolution in a Rock Joint Using a Complex Network Approach-Figures

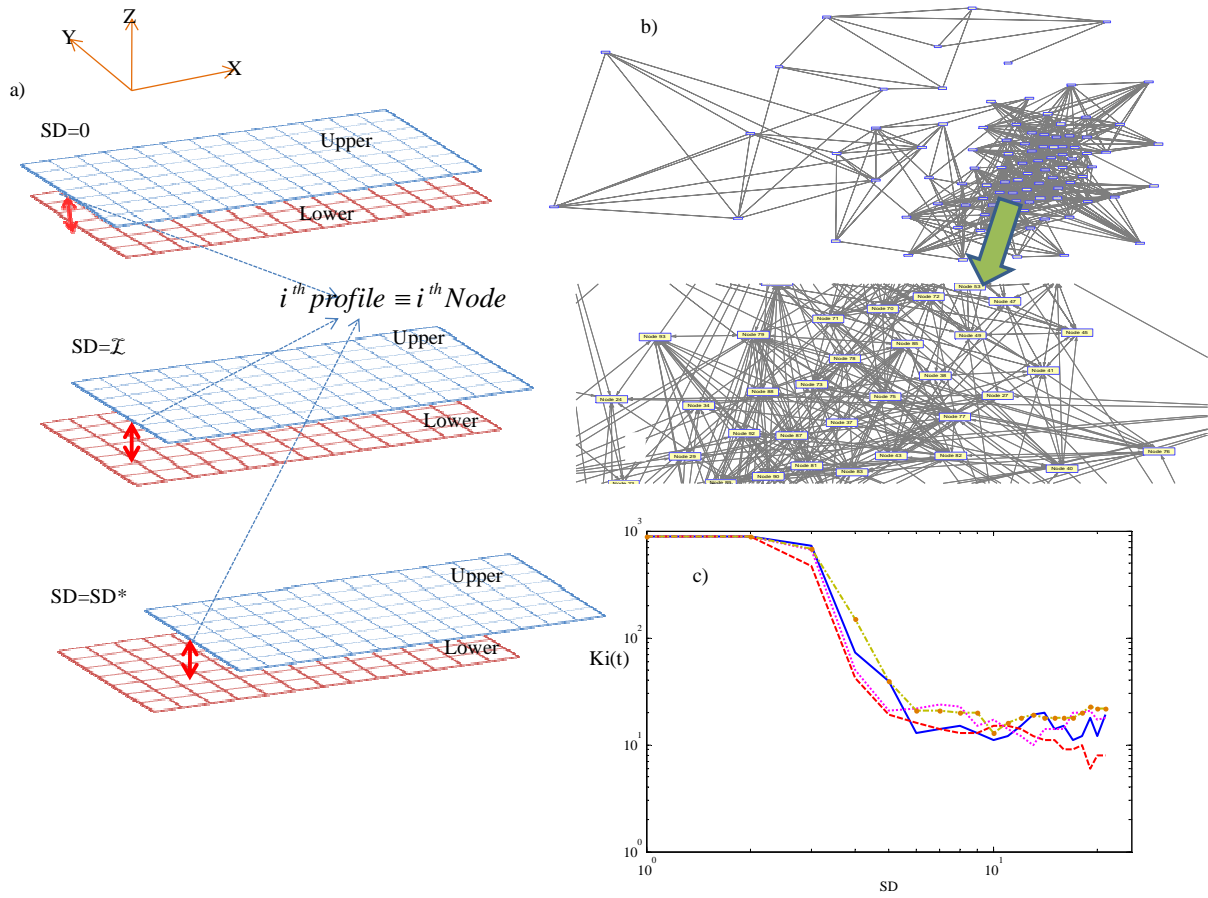


**Figure 1. a) Construction of a decaying complex network based on the measured apertures' profiles (the nodes references are coincided on the upper surface) ,b) Part of the created network (only first 100 nodes from 801 nodes) at 20 mm shear displacement (SD) and c) Evolutions of four nodes over the successive shear displacement (refer to the results section.)**



## Analysis of Aperture Evolution in a Rock Joint Using a Complex Network Approach-Figures

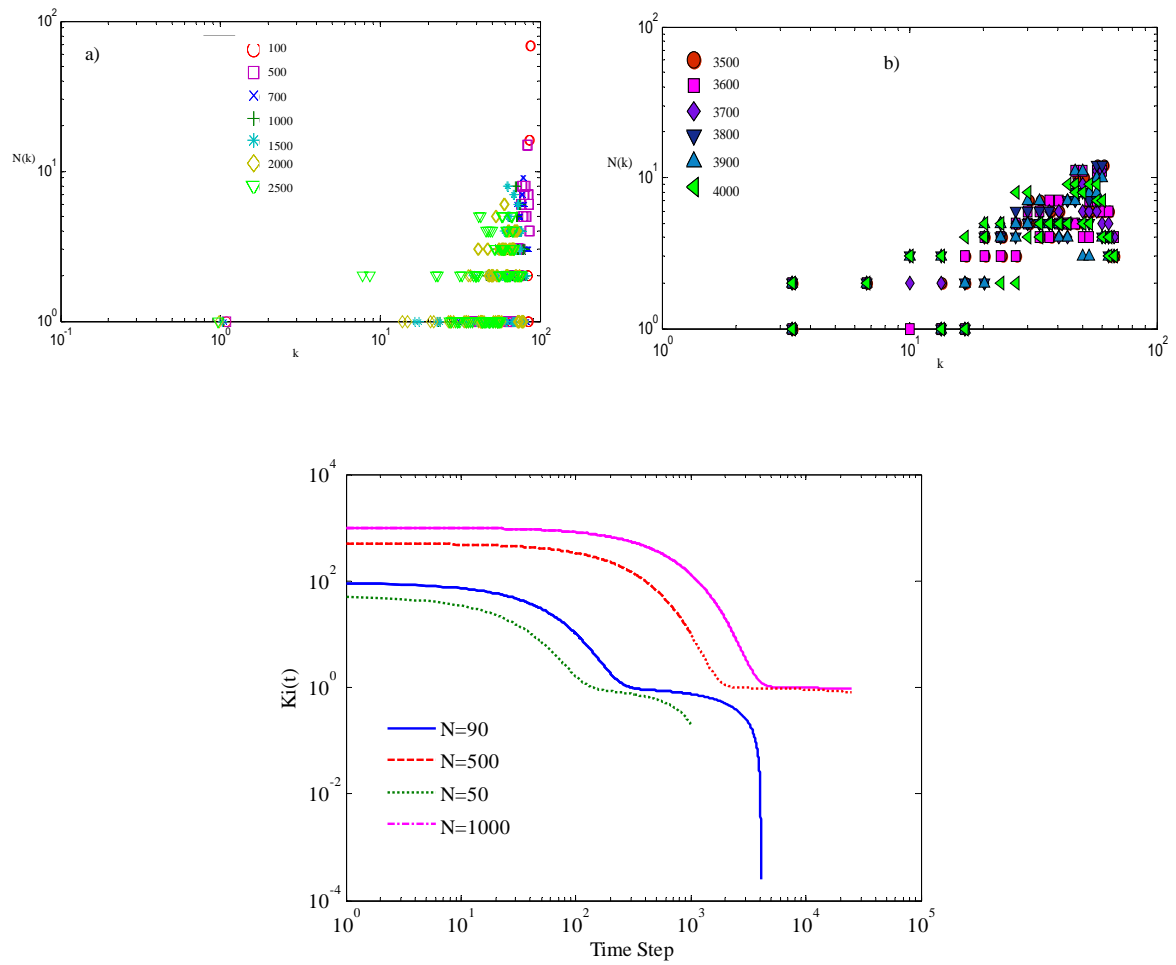


**Figure 2. a&b) the evolution of the edges distributions using the proposed algorithm and on  $N=90$ ; c) Analytical solution on several  $N$**

## Analysis of Aperture Evolution in a Rock Joint Using a Complex Network Approach-Figures

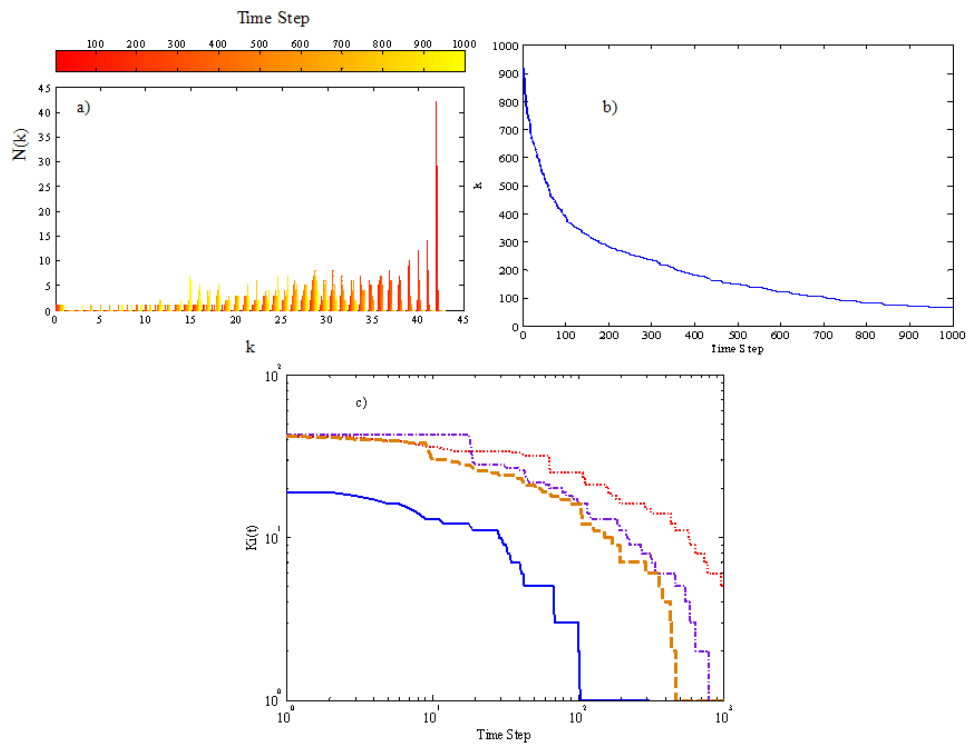
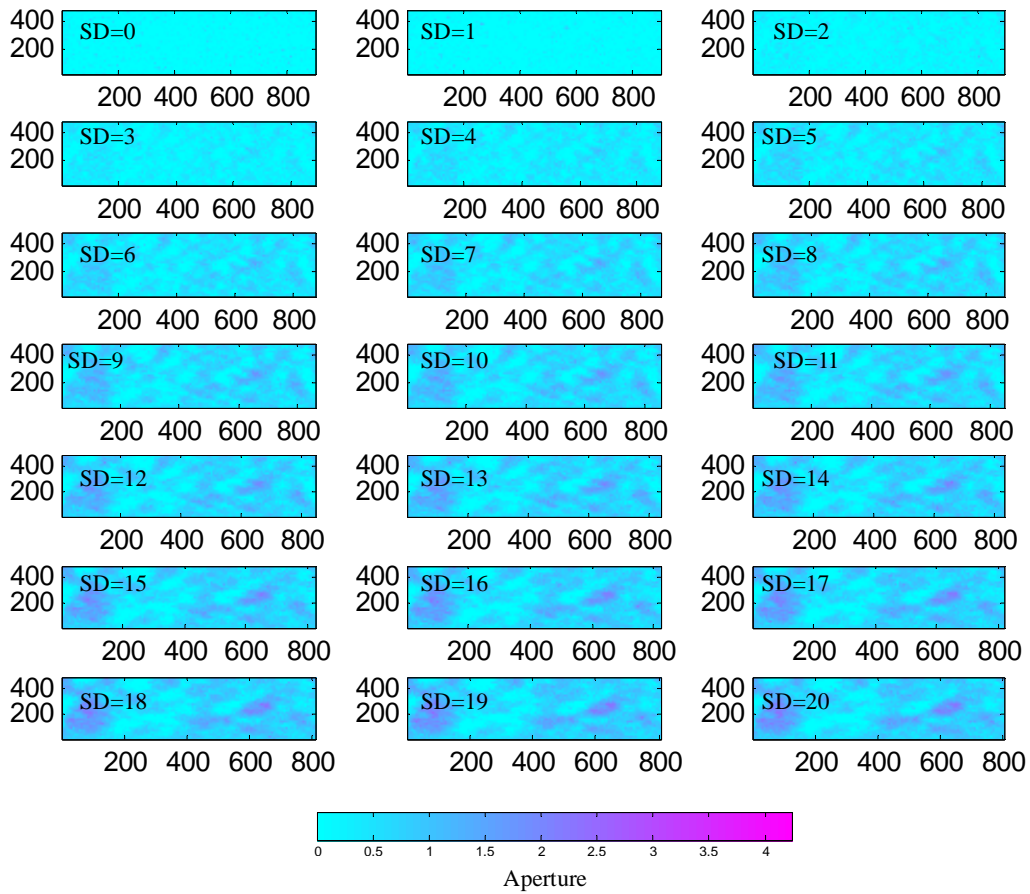


Figure 3. The evolution of the edges distributions and edge dependence using the proposed algorithm (a & b and c) on  $N=45$

## Analysis of Aperture Evolution in a Rock Joint Using a Complex Network Approach-Figures



**Figure 4.** The evolution of apertures 'patterns under successive shear displacements and 3 Mpa normal stresses (the axis show number of elements with a square element size of 0.2 mm)

## Analysis of Aperture Evolution in a Rock Joint Using a Complex Network Approach-Figures

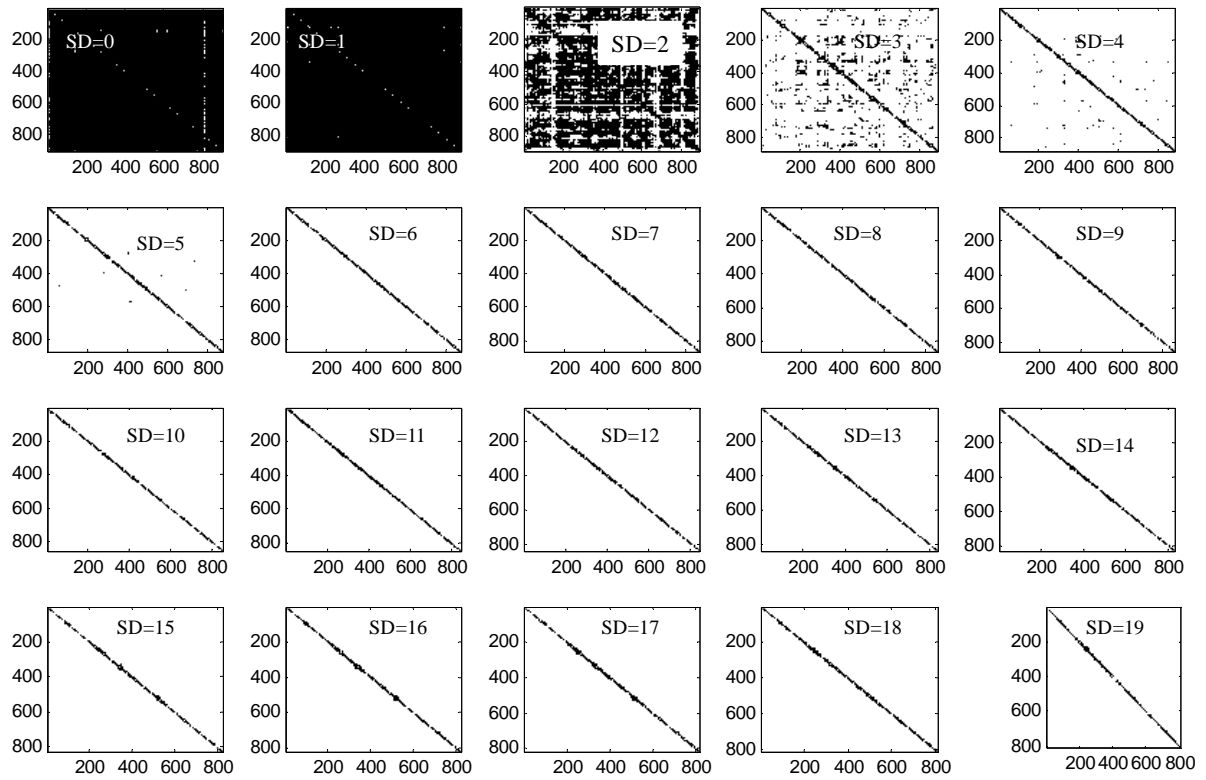


**Figure 5. The evolution of X-profiles networks (adjacency matrix visualization) using Euclidean distance and  $d \leq 5$**

## Analysis of Aperture Evolution in a Rock Joint Using a Complex Network Approach-Figures

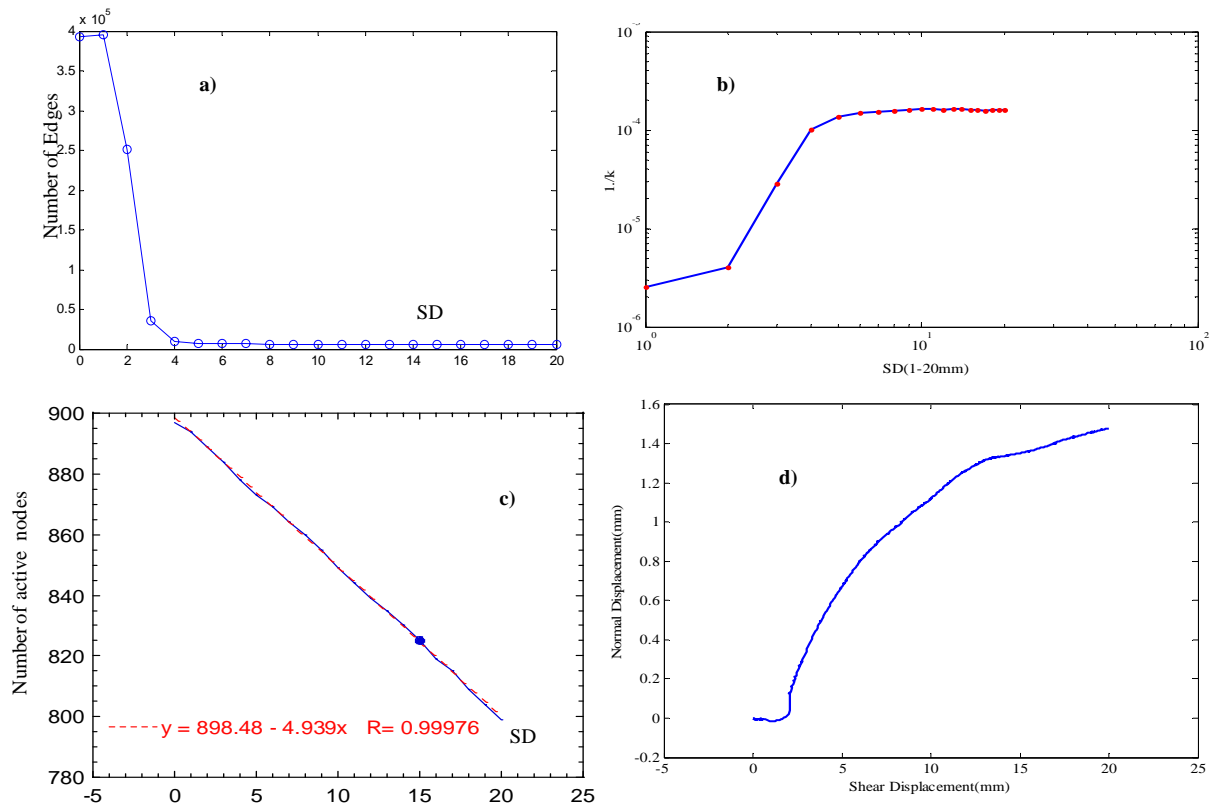


**Figure 6. Results on the X-profiles networks: a) Number of Edges -Shear displacement, b) Log-Log diagram of 1/Number Edges-Shear displacement, c) Number of active nodes (non-isolated vertices) -Shear displacement and d) Joint normal displacement-Shear displacement**

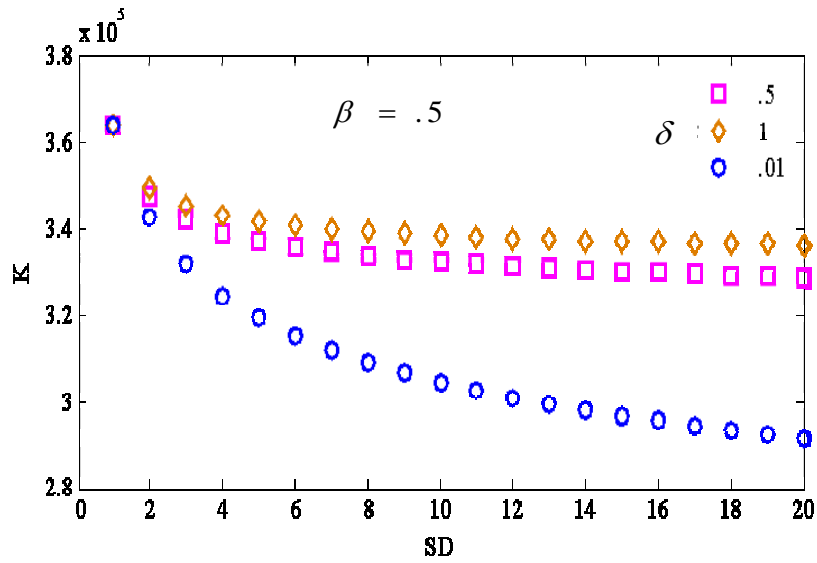


Figure 7. Approximation of Number of Edges (over the X-profiles networks) using a modified sigmoid function  $k = 2 \times 10^5 \times (1 + e^{-\beta(1 + \frac{LnSD}{1 + \delta LnSD})})$

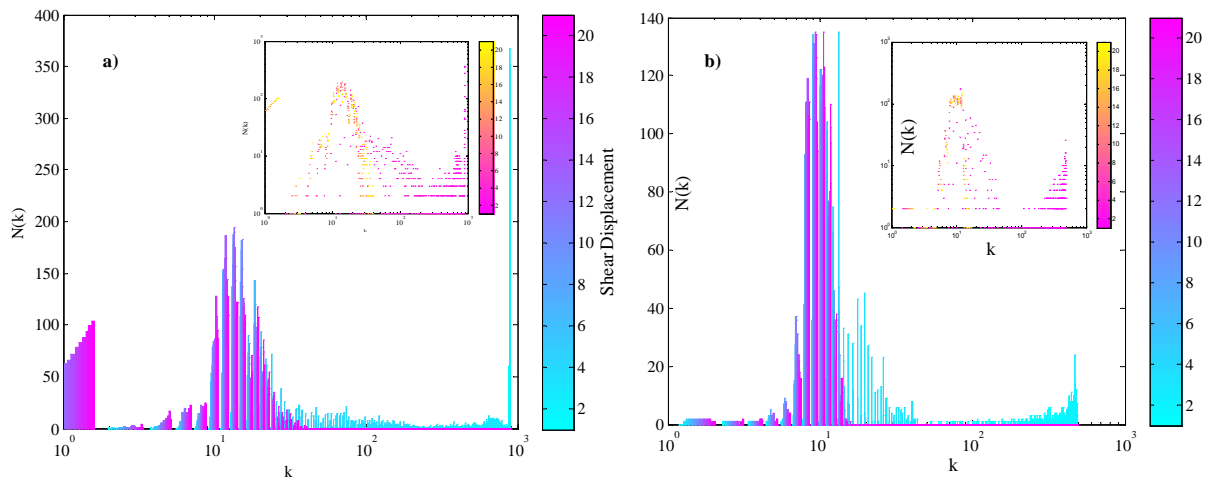
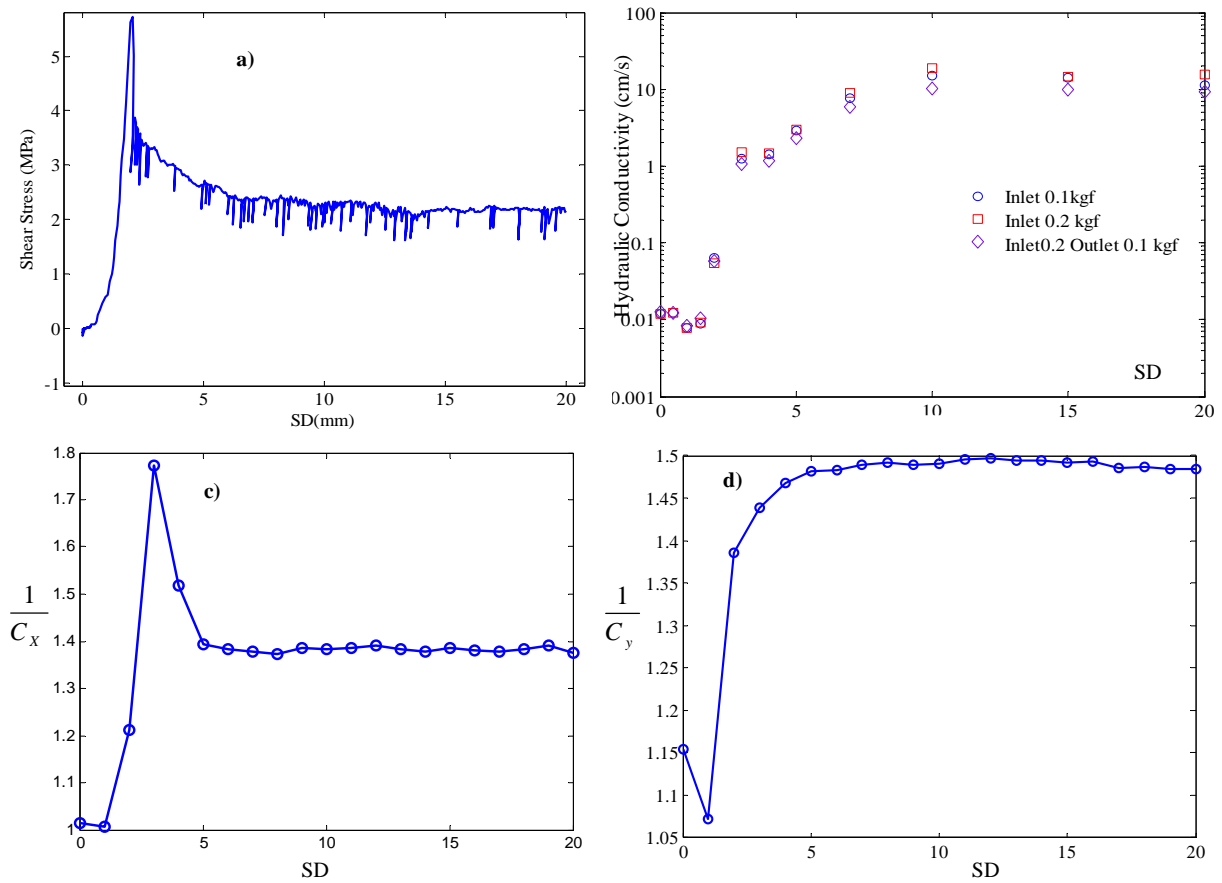


Figure 8. Frequency of nodes connectivity evolution over the shear displacements on: a) X-profiles and b) Y-profiles; Inset: results in log-log coordinate

**Analysis of Aperture Evolution in a Rock Joint Using a Complex Network Approach-Figures**



**Figure 9.a) Shear Stress -Shear Displacement (Normal Stress: 3Mpa), b) Hydraulic Conductivity - Shear Displacement associated with 3 different cases, c) &d) Inverse of Clustering Coefficients - Shear Displacement on the X and Y profiles ,respectively**

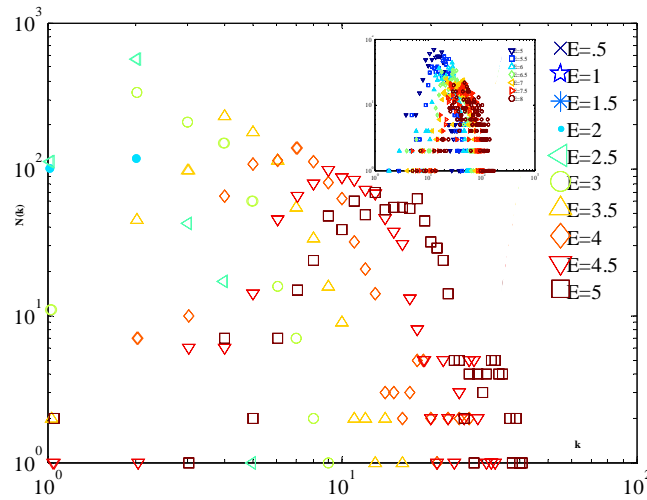


Figure 10. Effect of threshold variation ( $0.5 \leq \xi \leq 5$ ) at  $SD=20\text{mm}$  –Euclidean distance (inset:  $5 \leq \xi \leq 8$ )

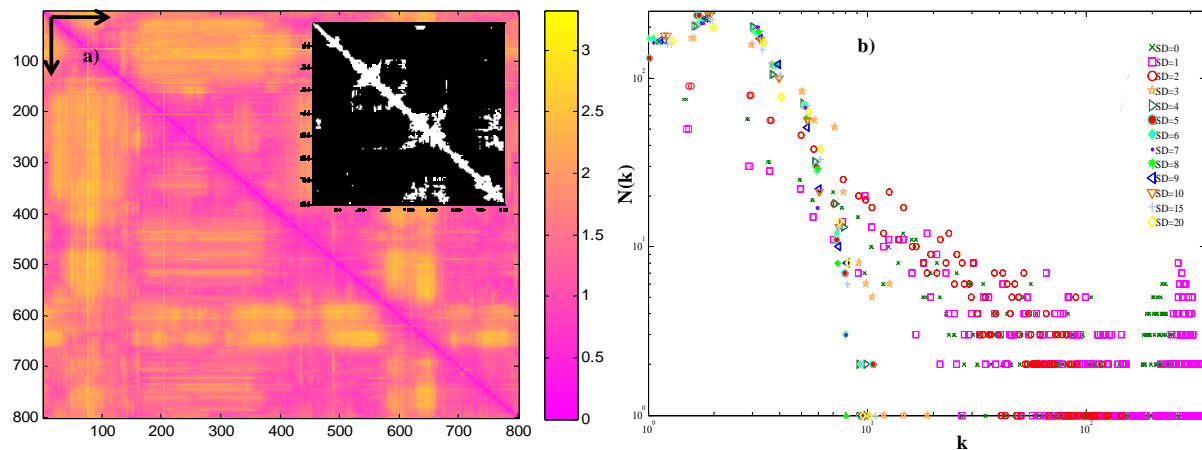
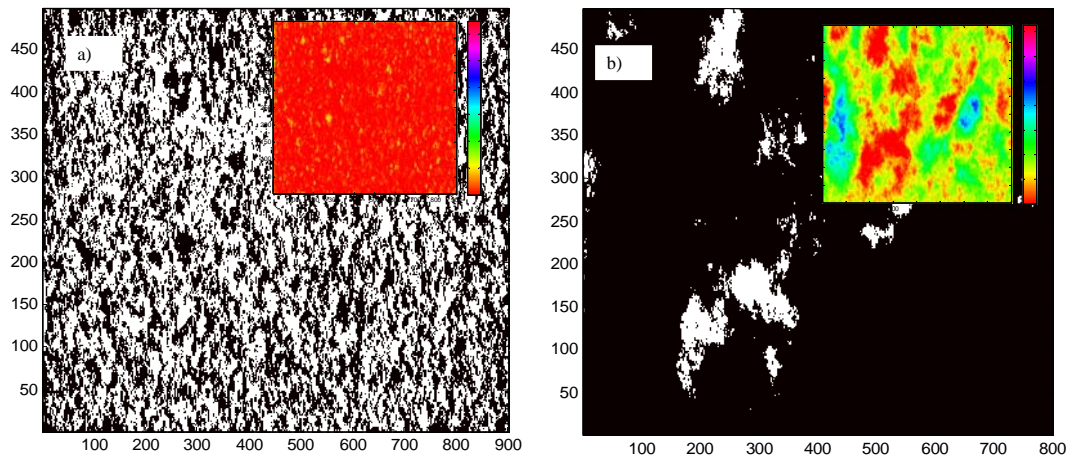


Figure 11. Results based on the Chebyshev distance: a) Distance matrix on X-profiles at 20 mm Shear Displacement (inset: Adjacency matrix of the proper network using  $d \leq 1$ ) and b) transition of edges distribution to a Gaussian distribution ( $d \leq .5$ )





**Figure12. Discrimination of Contact zones (white hues) at a) SD=0 and b) SD=20-Insents are overall apertures patterns.**

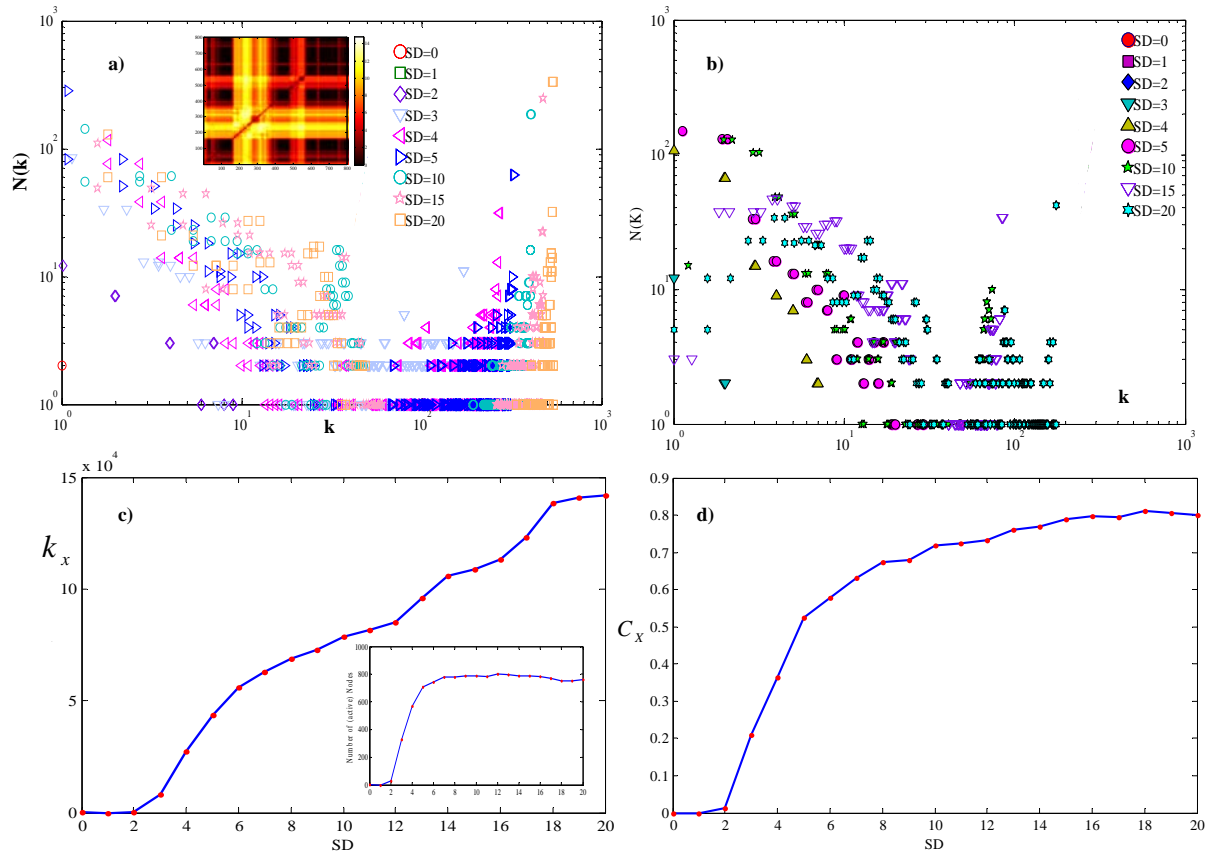


Figure13. Measurements on the contact zones (profile-profile) networks: a &b) Frequency of nodes connectivity evolution over the shear displacements on X-profiles (inset: appropriate distance matrix at 20 mm-SD) and Y-profiles, respectively, c) Growing of number of edges at X-profiles networks (inset: Number of active nodes evolving) and d) Clustering coefficient -Shear Displacement